Australian Journal of Basic and Applied Sciences

2020 October; 14(10): pages 35-47
DOI: 10.22587/ajbas.2020.14.10.5

Original paper AENSI Publications

Aluminium corrosion inhibition in 1M HCl by nicotinamide: gravimetric, thermodynamic, kinetic and QSPR studies

Mamadou Yeo[1], Victorien Kouakou[1], Mougo André Tigori[2], Paulin Marius Niamien[1]*, Albert Trokourey[1]

[1]Laboratory of Constitution and Reaction of Matter, UFHB, Abidjan-Cocody, 22 BP 582 Abidjan 22.
[2]UFR Environnement, UJLoG, BP 150 Daloa, Côte d'Ivoire

Correspondence Author: Niamien Paulin Marius, Laboratory of Constituton and Reaction of Matter, UFHB, Abidjan-Cocody, 22 BP 582 Abidjan 22.
E-mail:- *niamienfr@yahoo.fr*

Received date: 22 August 2020, Accepted date: 29 October 2020, Online date: 15 November 2020

Copyright: © 2020 Mamadou Yeo et al, This is an open-access article distributed under the terms of the Creative Commons Attribution License, which permits unrestricted use, distribution, and reproduction in any medium, provided the original author and source are credited.

Abstract

Background: Corrosion inhibitors are chemical compounds used in small quantities in liquid or gas to decrease the corrosion rate of a material. A perusal of literature shows that organic compounds have often been tested as corrosion inhibitors due to their capacity to reduce this phenomenon.
Objective: This work stands for the study of Nicotinamide (NTA) behaviour as an aluminium corrosion inhibitor in 1M HCl.
Methods: The experimental studies were carried out by gravimetry and the obtained results gave access to the corrosion rate and the inhibition efficiency. DFT calculations performed using Gaussian 09 allowed determining the molecular parameters. QSPR studies allowed the establishment of mathematical formulas to correlate corrosion inhibition with molecular parameters.
Results: The obtained results show that the inhibition efficiency increases with increasing concentration in (NTA) but decreases when temperature increases. The molecule adsorbs on the aluminium surface according to the modified Langmuir isotherm known as Villamil isotherm. Adsorption and activation thermodynamic functions were determined. The metal dissolution kinetic law was established. The global molecular descriptors such as the frontier energies (E_{HOMO}, E_{LUMO}), the energy gap (ΔE), the dipole moment (μ), the chemical potential (μ_P), the chemical hardness (η) and the global nucleophilicity (ω) were obtained. The local descriptors known as Fukui functions (f_k^α), dual descriptors (Δf_k^α) and ($\Delta\omega_k^\alpha$) were also determined. Mathematical relations correlate well the molecular descriptors with the corrosion inhibition efficiency.

Keywords: Aluminium, hydrochloric acid, nicotinamide, corrosion inhibition, mass loss, kinetic law, DFT, molecular descriptor, QSPR.

INTRODUCTION

Aluminium is nowadays an economic competitor in engineering applications. The metal (Polnear, 1995) has many properties that can be used precisely in applications including household foils, construction material, transportation and aerospace applications. The properties of aluminium (Davis, 1999) which justify its widespread usage are the following: lightness, high resistance to corrosion, excellent conductor of heat and electricity, nontoxicity, etc. Though aluminium resists to its destruction due to the presence of an oxide film on its surface, in some environmental conditions it is corroded. Corrosion is a natural process that converts the metal into a more stable form such as its oxide. This process occurs once the oxide film has been destroyed. To combat corrosion (Obot et al., 2009; khaled and Al-Qahtani, 2009; Abdallah et al., 2010), the use of organic molecules with heteroatoms is one of the best ways. Generally, organic compounds with nitrogen, sulphur or oxygen atoms and /or π–bonds in their structure are efficient. Actually, drugs are used as corrosion inhibitors for metals in aggressive environment. So, antibacterial drugs (Naqui I. et al., 2011; Singh A. K. et al., 2011; Kumar S. H. and Karthikeyan S., 2012), antibiotics (Abdallah M.,2004), cephalosporins (Ameh P. O. and Sami U.M., 2015) have been tested in the case of mild steel or aluminium corrosion in acidic media.

Citation: Mamadou Yeo et al., 2020. Aluminium corrosion inhibition in 1M HCl by nicotinamide: gravimetric, thermodynamic, kinetic and QSPR studies. Australian Journal of Basic and Applied Sciences, 14(10): 35-47. DOI: 10.22587/ajbas.2020.14.10.5

These studies focus on the effects of the NTA on aluminium corrosion in1M HCl. The mass loss technique was used to determine the type of adsorption. Adsorption and activation thermodynamic parameters (free enthalpy variation, enthalpy variation and entropy variation) were then determined. The studies also aim to elucidate the kinetics of the metal dissolution. In order to shed more light on the correlation between the inhibition efficiency of NTA and some sets of molecular parameters, DFT method and QSPR approach were used.

MATERIALS AND METHODS

Aluminium specimens

Aluminium samples of purity 99.5%, in the form of rod with 10 mm of length and 2 mm in diameter were used.

The studied molecule

The structure of Nicotinamide (NTA) (chemical formula: $C_6H_6N_2O$) is given below (Fig. 1).

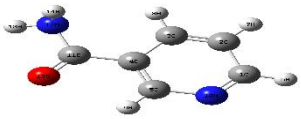


Fig.1: Nicotinamide's optimized structure using B3LYP/6-31G (d)

Solutions

HCl of purity 37%, from Merck was used to prepare blank of 1M. Nicotinamide (purity≥ 99%) from Merck was used to prepare solutions of concentrations ranging from 0.13 to 0.53mM.

Mass loss studies

Prior to the experiment, the sample was abraded with papers of grade ranging from 200 to 1000. It was then washed several times with double distilled water and with acetone and dried in a desiccator. After weighing accurately, using analytical balance (precision $\pm$ 0.1 mg), the sample was immersed in 50 mL aerated 1.0 M solution without or with the desired concentration of NTA. After 1 h, the specimen was retrieved from the solution, washed abundantly with water, dried and weighed accurately. The test was repeated at different temperatures ranging from 298 to 323K, using different samples. The corrosion rate value was calculated, using the equation below:

$$w = \frac{m_0 - m}{St} \quad (1)$$

Where m_0 is the mass of the sample before the test, m is the mass of the sample after the test, S is the total area of the sample; t is the corrosion time and w, the corrosion rate.

The inhibition efficiency EI (%) was calculated using the equation below:

$$IE(\%) = \frac{W_0 - W}{W_0} \times 100 \quad (2)$$

Where w_0 (w) is the corrosion rate of the sample in the blank (and in the blank containing NTA).

Kinetics studies

The experiments were realised at different times ranging from 0.5 to 4.5 h and at different temperatures.

Density Functional Theory calculations

Density functional Theory method B3LYP/6-31 G (d), implemented in Gaussian 09 program (Frisch M. J. et al., 2009) was used to optimized NTA molecule.

The quantum calculations were utilized to determine quantum parameters such as the energy of the highest occupied molecular orbital (E_{HOMO}), the energy of the lowest unoccupied molecular orbital (E_{LUMO}) and the dipole moment (μ), essential to access to the corrosion inhibition mechanism of NTA.

Global parameters

The global parameters derived from the first two parameters are the HOMO-LUMO gap (ΔE), the chemical hardness (η) and softness (σ), the chemical potential (μ_p) and the electrophilicity index (ω). These parameters are given by the equations below:

$$\Delta E = E_{LUMO} - E_{HOMO} \quad (3)$$

$$\eta = \frac{1}{2}(-E_{HOMO} + E_{LUMO}) \quad (4)$$

$$\sigma = \frac{1}{\eta} \quad (5)$$

$$\mu_P = \frac{1}{2}(E_{HOMO} + E_{LUMO}) \quad (6)$$

$$\omega = \frac{\mu_P^2}{2\eta} \quad (7)$$

Citation: Mamadou Yeo et al., 2020. Aluminium corrosion inhibition in 1M HCl by nicotinamide: gravimetric, thermodynamic, kinetic and QSPR studies. Australian Journal of Basic and Applied Sciences, 14(10): 35-47. DOI: 10.22587/ajbas.2020.14.10.5

Local parameters

The local parameters including Fukui functions and dual functions were also determined to give insight on the molecular nucleophilic and electrophilic characters of NTA. The electronic density $\rho(r)$, the first local molecular parameter in DFT is defined as:

$$\rho(r) = \left(\frac{\partial E}{\partial v(r)}\right)_N \quad (8)$$

The chemical reactions in general involve a change in electron density, what explains the use of the Fukui function (Geerling P. and al., 2007) instead of the electronic density. The Fukui function is given by the following equation:

$$f^{\alpha}(r) = \left(\frac{\partial \rho(r)}{\partial N}\right)^{\alpha}_{v(r)} = \left(\frac{\partial \mu_P}{\partial v(r)}\right)^{\alpha}_{N} \qquad (\alpha = +or -) \quad (9)$$

In this relation, N is the total number of electrons and $v(r)$ is the constant external potential.

The condensed Fukui functions or condensed reactivity indicators which are apply to an atom within a molecule rather than a point in three-dimensional space, are calculated using a procedure (Yang W. and Mortier W. J., 1986) based on a finite difference method:

$$f_k^+ = q_k(N+1) - q_k(N) \quad (10)$$

$$f_k^- = q_k(N) - q_k(N-1) \quad (11)$$

Where q_k represents the electronic population of atom k in the molecule. The functions f_k^+ and f_k^- are relevant to a nucleophilic and an electrophilic attack.

Actually a descriptor called dual descriptor has been proposed (Morell C. and al., 2005 and 2006) to define the difference between the Fukui functions:

$$\Delta f_k = f_k^+ - f_k^- \quad (12)$$

The site favours a nucleophilic attack for $\Delta f_k > 0$ and an electrophilic attack for $\Delta f_k < 0$.

Combining the local philicity concept (Chattaraj et al., 2003) and that of the dual descriptor (Morell C. and al., 2005 and 2006) a multiphilic descriptor is proposed:

$$\Delta\omega = \omega(f_k^+ - f_k^-) \quad (13)$$

QSPR studies

Quantitative Structure-Property Relationships (QSPR) is a mathematical approach which attemps to relate the structure derives features of a compound to its biological or physicochemical activity.

In order to link some sets of composite indexes (quantum chemical and reactivity parameters) with the experimental corrosion inhibition efficiency, a non-linear model was used (Lukovits et al., 3003). This model is given as follows:

$$IE(\%) = \frac{(Ax_j+B)C_i}{1+(Ax_j+B)C_i} \times 100 \quad (14)$$

In the above equation, A and B are real constants, determined by solving the system of simultaneous equations obtained from different values of inhibitor concentration C_i and x_j is a quantum chemical parameter.

RESULTS AND DISCUSSION

Mass loss results

Results obtained through mass loss experiments reveal a decrease in corrosion inhibition rate values when the concentration in NTA increases. Consequently, the corrosion inhibition efficiency increases with increase in the concentration (Fig. 2).

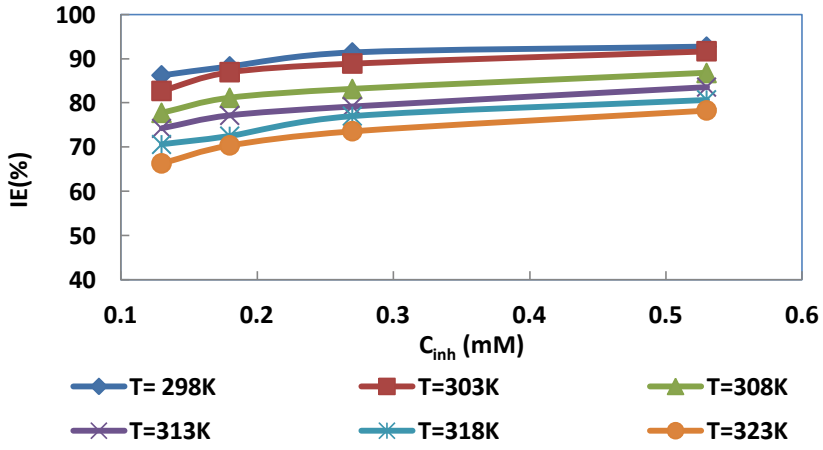


Fig. 2: IE (%) versus C_{inh} for different temperatures.

We note that this behaviour which is the same for all the range of temperatures could be attributed (Obi-Egbedi N. O., 2011) to the enhancement of the adsorption strength with increase in inhibitor's concentration. Aluminium corrosion inhibition in solutions

Citation: Mamadou Yeo et al., 2020. Aluminium corrosion inhibition in 1M HCl by nicotinamide: gravimetric, thermodynamic, kinetic and QSPR studies. Australian Journal of Basic and Applied Sciences, 14(10): 35-47. DOI: 10.22587/ajbas.2020.14.10.5

containing NTA decreases with increasing temperature (Fig. 3). This results could be explained by a decrease (Eddy N. O. and al., 2015) in adsorption strength or by a desorption of NTA molecules from the aluminium surface.

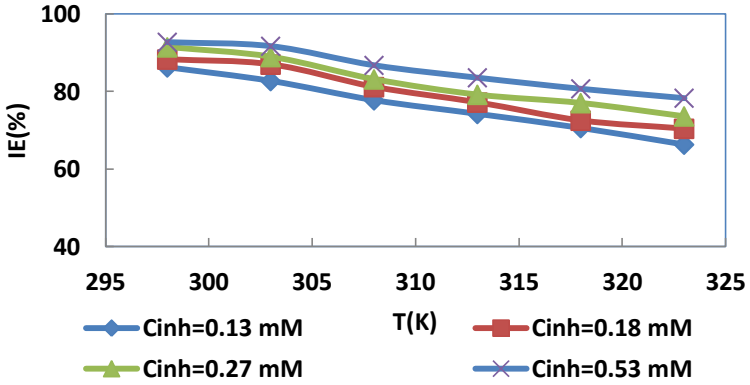


Fig. 3: IE (%) versus temperature for different concentrations in NTA

Adsorption and thermodynamic considerations

Corrosion inhibitors generally protect metals in aggressive media by adsorbing themselves on their surfaces. This substitutional adsorption process is given by the equation below:

$$Org_{(sol)} + xH_2O_{(ads)} \rightleftarrows Org_{(ads)} + xH_2O_{(sol)} \quad (15)$$

Informations on the adsorption of an organic compound onto a metal surface can be obtained, using adsorption isotherms. So, we tried to fit experimental data to various adsorption isotherms models such as Langmuir, El-Awady, Freundlich, etc. All these isotherms (Sahin M. et al., 2002) are of general form:

$$f(x,\theta)\exp(-2\alpha\theta) = K_{ads}C_i \quad (16)$$

Where $f(x,\theta)$is the configural factor, θ is the rate of covered surface, α the molecular interactions parameter (positive values indicate attraction forces while negative ones are synonym of repulsive forces) $K_{ads}$is the equilibrium adsorption constant, x is the size factor ratio (number of water molecules replaced by one inhibitor molecule) and C_i is the inhibitor constant.

Villamil isotherm

Although the Langmuir's isotherm is the best suited to the experimental data, some of the hypotheses that led to its development are not respected.

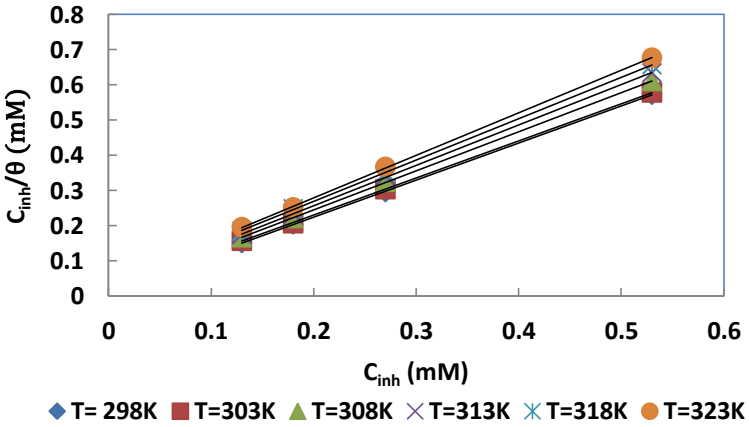


Fig. 4: Langmuir isotherm plots for NTA adsorption onto aluminium in 1M HCl

The suitable adsorption model is then the modified Langmuir isotherm (Villamil et al., 1999) giving by the following equation:

$$\frac{C_{inh}}{\theta} = \frac{n}{K_{ads}} + nc_{inh} \quad (17)$$

Where n is the slope of the plot and $n\theta$ is the effective covered surface fraction of the metal. The Villamil isotherm parameters are listed in Table 1.

Citation: Mamadou Yeo et al., 2020. Aluminium corrosion inhibition in 1M HCl by nicotinamide: gravimetric, thermodynamic, kinetic and QSPR studies. Australian Journal of Basic and Applied Sciences, 14(10): 35-47. DOI: 10.22587/ajbas.2020.14.10.5

Table1: Parameters of Langmuir modified adsorption isotherm

T(K)	Equation	R^2	$K_{ads}(M^{-1})$	ΔG^0_{ads} (kJmol^{-1})	ΔH^0_{ads} (kJmol^{-1})	ΔS^0_{ads} (Jmol^{-1}K^{-1})
298	$C_{inh}/\theta = 1.052C_{inh} + 0.0157$	0.999	67006.4	-37.465	-25.41	40.4
303	$C_{inh}/\theta = 1.055C_{inh} + 0.0187$	1.000	56417.1	-37.660		
308	$C_{inh}/\theta = 1.110C_{inh} + 0.0232$	1.000	47844.8	-37.860		
313	$C_{inh}/\theta = 1.147C_{inh} + 0.0277$	0.999	41407.9	-38.099		
318	$C_{inh}/\theta = 1.176C_{inh} + 0.0336$	0.999	35000.0	-38.263		
323	$C_{inh}/\theta = 1.206C_{inh} + 0.0399$	0.999	30225.6	-38.471		

Variation of adsorption free enthalpy ΔG^0_{ads} is linked to adsorption constant K_{ads} by:

$$\Delta G^0_{ads} = -RTln(55.5 \times K_{ads}) \quad (18)$$

In this equation, R is the universal constant, T is the absolute temperature and 55.5 represents water concentration in mol.L^{-1}. Variation of adsorption enthalpy (ΔH^0_{ads}) and entropy (ΔS^0_{ads}) were obtained from the equation below:

$$\Delta G^0_{ads} = \Delta H^0_{ads} - T\Delta S^0_{ads} \quad (19)$$

These parameters are determined using the plot of variation of free enthalpy versus temperature (Fig. 5).

The results show that ΔG^0_{ads} is negative indicating a spontaneous adsorption process. The values range from -37.5kJ to -38.5 kJ showing (Umoren S. A. et al., 2006) the existence of the two types of adsorption process. The variation of enthalpy ΔH^0_{ads} is negative indicating an exothermic process; it's absolute value (25.41 kJ.mol^{-1}) is lower than 40 kJ.mol^{-1} indicating (Badiea A. M. and Mohana K. N., 2009) a physisorption process predominance.

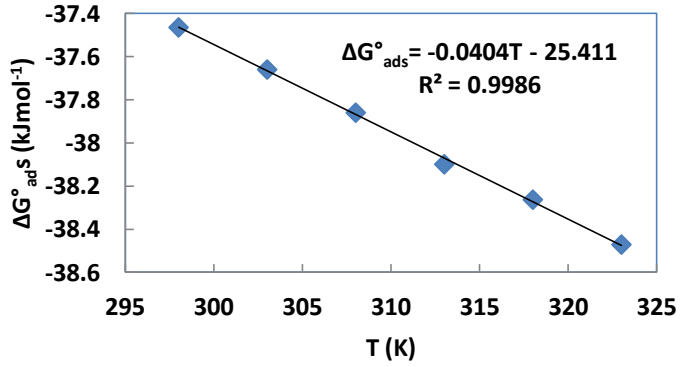


Fig. 5: Variation of free adsorption energy versus temperature

The variation of entropy (ΔS^0_{ads}) is positive, showing an increase in disorder due probably to desorption of water molecules with increasing temperature.

Adejo-Ekwenchi isotherm

In order to bring light on the adsorption type, we used Adejo-Ekwenchi isotherm. This isotherm (Adejo O. O. and Ekwenchi M. M., 2014) is described by the following equation:

$$log\left(\frac{1}{1-\theta}\right) = logK_{AE} + blogC_{inh} \quad (20)$$

Where K_{AE} and b are the isotherm parameters and C_{inh} is the inhibitor concentration. Fig. 6 gives the plots of the isotherm for different temperatures.

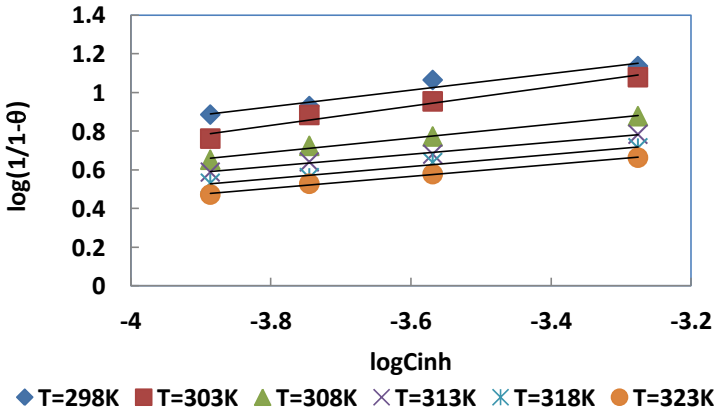


Fig. 6: Adejo-Ekwenchi isotherm plots for NTA in 1M HCl

Citation: Mamadou Yeo et al., 2020. Aluminium corrosion inhibition in 1M HCl by nicotinamide: gravimetric, thermodynamic, kinetic and QSPR studies. Australian Journal of Basic and Applied Sciences, 14(10): 35-47. DOI: 10.22587/ajbas.2020.14.10.5

All the calculated parameters of the described isotherm are listed in Table 2.

Table 2: Adejo-Ekwenchi isotherm parameters

T(K)	Equation	R^2	b	K_{AE}
298	$\log(1/1-\theta) = 0.4309 log C_{inh} + 2.5639$	0.9465	0.4309	366.3
303	$\log(1/1-\theta) = 0.4971 log C_{inh} + 2.7189$	0.9705	0.4970	523.5
308	$\log(1/1-\theta) = 0.3577 log C_{inh} + 2.0512$	0.9910	0.3577	112.5
313	$\log(1/1-\theta) = 0.3133 log C_{inh} + 1.8075$	0.9940	0.3133	64.2
318	$\log(1/1-\theta) = 0.3108 log C_{inh} + 1.7362$	0.9860	0.3108	54.5
323	$\log(1/1-\theta) = 0.3070 log C_{inh} + 1.6718$	0.9950	0.3070	47.0

In Table 2, we can observed that the temperature ranges from 298K to 303 K; we have an increase in b and K_{AE}, indicating an increase in adsorption strength what is generally associated with chemisorption. For temperatures range from 303 to 323K, we observed a decrease in b and K_{AE} values, showing a physical adsorption character. So, we can note the existence of the two types of adsorption but a predominance of physical adsorption.

Activation and thermodynamic functions

The activation energyE_a, the variation of activation enthalpy ΔH_a^* and entropy ΔS_a^* were deduced using the following equations:

$$logw = logA - \frac{E_a}{2.303RT} \quad (21)$$

$$log\left(\frac{W}{T}\right) = log\left(\frac{R}{\aleph h}\right) + \left(\frac{\Delta S_a^*}{2.303R}\right) - \left(\frac{\Delta H_a^*}{2.303RT}\right) \quad (22)$$

Where w, A, R, T, $\aleph$ and h are respectively the corrosion rate, the frequency factor, the perfect gas constant, the absolute temperature, the Avogadro constant and the Planck constant.

Fig. 7 shows $logW$ versus 1/T. We have straight lines with slopes $(\frac{E_a}{2.303R})$ and intercepts $logA$.

To access to the values of variation of enthalpy ΔH_a^* and entropyΔS_a^* , we have represented log (W/T) versus 1/T. We obtained straight lines (Figure 8) with slopes $\left(-\frac{\Delta H_a^*}{2.303R}\right)$ and intercepts [$log\left(\frac{R}{\aleph h}\right) + \left(\frac{\Delta S_a^*}{2.303R}\right)$], which allow us to deduce the desired parameters.

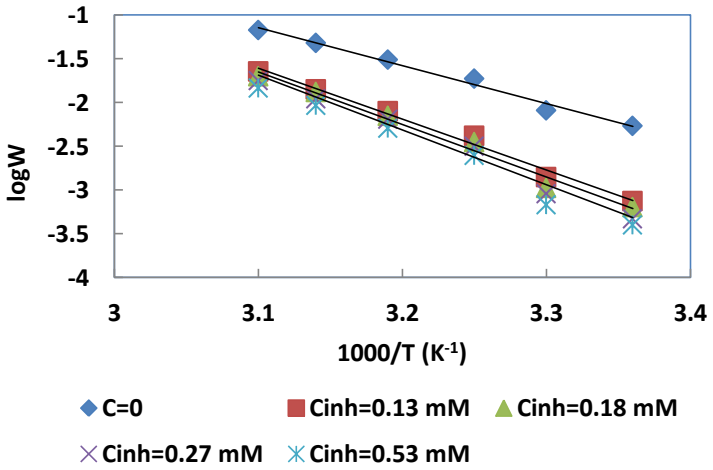


Fig. 7: logW versus 1/T for different concentrations

Citation: Mamadou Yeo et al., 2020. Aluminium corrosion inhibition in 1M HCl by nicotinamide: gravimetric, thermodynamic, kinetic and QSPR studies. Australian Journal of Basic and Applied Sciences, 14(10): 35-47. DOI: 10.22587/ajbas.2020.14.10.5

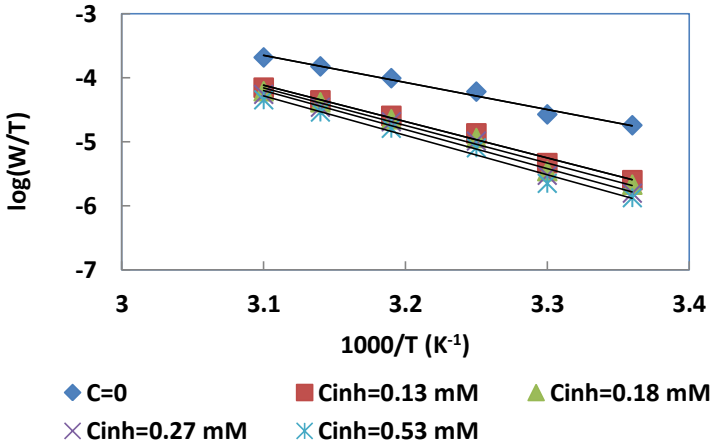


Fig. 8: log (W/T) versus 1/T for different concentrations

Table 3 contains all the calculated activation parameters.

Table3: Dissolution parameters for aluminium in 1M HCl with or without NTA

Concentration (mM)	$E_a\ (kJmol^{-1})$	$\Delta H_a^*\ (kJmol^{-1})$	$\Delta S_a^*\ (Jmol^{-1}K^{-1})$
Blank	83.2	80.8	-16.9
0.13	111.2	108.8	61.0
0.18	115.0	112.6	72.2
0.27	119.2	116.9	84.4
0.53	120.0	117.6	85.0

The apparent activation (E_a) energy increases with the concentration of NTA, what indicates (Fouda et al., 2006) a physical adsorption trend.

The positive sign of variation of enthalpy (ΔH_a^*) both in the absence and presence of NTA shows the endothermic nature of aluminium dissolution process. It is clear from Table 3 that (ΔH_a^*) increases with increasing concentration in NTA, indicating (Ebenso E. E. and Obot I.B., 2010) the difficulty of aluminium dissolution. The variation of activated entropy (ΔS_a^*) is positive in presence of NTA, showing an increase in disorder, probably due to desorption of adsorbed species; this situation is also indicative (Obi-Egbedi N. O. and Obot I. B., 2011) of the fact that the activated complex results from an association instead of a dissociation. To acess information concerning the kinetic of the dissolution of aluminium in the 1 M HCl solution, both in presence of NTA or not, we have studied the evolution of the sample mass along time. The dependence of the corrosion process with time has been evaluated under ambient temperature by fitting experimental data into to different kinetic models:

Order 0: $m_0 - m = kt$ (23)

Order 1: $ln\frac{m_0}{m} = kt$ (24)

Order 2: $\frac{1}{m} - \frac{1}{m_0} = kt$ (25)

Fig. 9 A, 9 B and 9 C give the different plots corresponding to the three kinetics models.

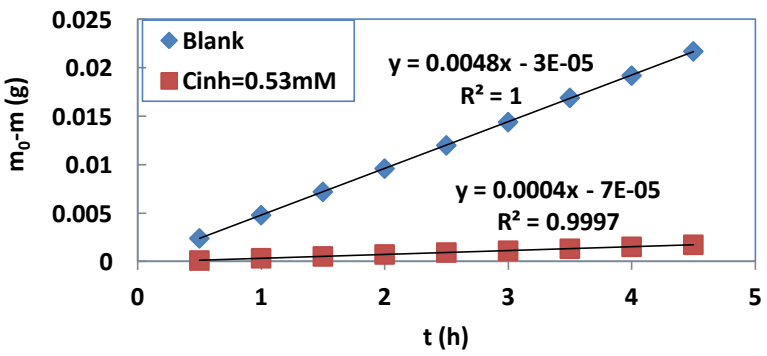


Fig.9 A: Plots relative to the zero order kinetic law at T = 298K

Citation: Mamadou Yeo et al., 2020. Aluminium corrosion inhibition in 1M HCl by nicotinamide: gravimetric, thermodynamic, kinetic and QSPR studies. Australian Journal of Basic and Applied Sciences, 14(10): 35-47. DOI: 10.22587/ajbas.2020.14.10.5

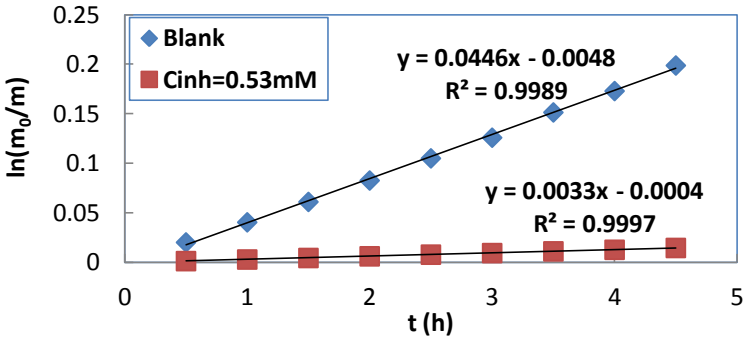


Fig. 9 B: Plots relative to the first order kinetic law at T = 298K

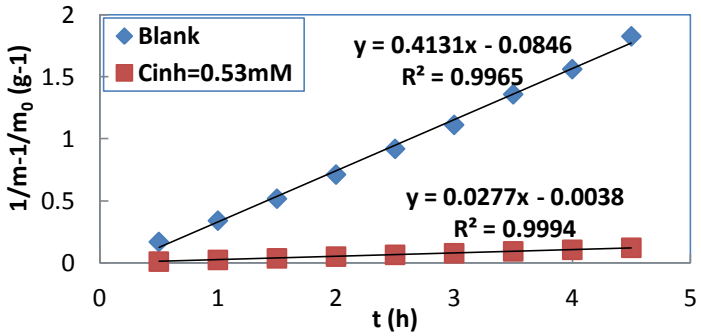


Fig. 9 C: Plots relative to the second order kinetic law at T = 298K

All the curves are straight lines, what indicates that the presence of the inhibitor does not change the kinetic of the aluminium dissolution reaction even if the rate of corrosion is considerably reduced. The resulting linear correlation coefficients and the different intercepts show that the metal dissolution obeys the zero order kinetic process (R^2 = 1 and intercept very close to the origin). All the calculated parameters are given in Table 4.

Table 4: Parameters for the different kinetic processes at T = 298K.

Kinetic law	Inhibitor concentration(mM)	R^2	Slope	Intercept
Zero order	0.00	1	4.8010^{-3}	-3.010^{-5}
	0.53	0.9997	4.0010^{-4}	-7.010^{-5}
First order	0.00	0.9989	4.4610^{-2}	-4.810^{-3}
	0.53	0.9997	3.3010^{-3}	-4.010^{-4}
Second order	0.00	0.9965	4.1310^{-1}	-8.510^{-2}
	0.53	0.9994	2.7710^{-2}	-3.810^{-3}

In Table 4, the units are:

- For the slopes: zero order ($g.h^{-1}$), first order (h^{-1}) and second order ($g^{-1}.h^{-1}$);
- For the intercepts: zero order (g), first order (no unit) and second order (g^{-1}).

The activation energy can be obtained using the equation below:

$$E_a = \frac{RT_1T_2}{T_2 - T_1} ln\left(\frac{k_{T_2}}{k_{T_1}}\right) \qquad (26)$$

Where k_{T_1} and k_{T_2} are respectively the constant rates, slopes of the straight lines obtained for the kinetic of zero order at the two temperatures T_1 = 298K and T_2 = 318K.

In order to access to the activation energy, we represent in Fig. 10, mass loss versus time at T = 318K.

Citation: Mamadou Yeo et al., 2020. Aluminium corrosion inhibition in 1M HCl by nicotinamide: gravimetric, thermodynamic, kinetic and QSPR studies. Australian Journal of Basic and Applied Sciences, 14(10): 35-47. DOI: 10.22587/ajbas.2020.14.10.5

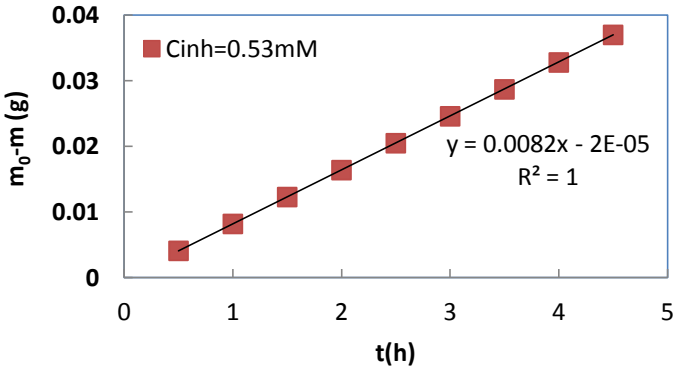


Fig. 10: Plots relative to the zero order kinetic law at T = 318K

We observe that the value of activation energy for C_{inh} = 0.53mM, using equation 21 (E_a =120 kJ.mol^{-1}) and that obtained from equation 26 (E_a = 118.93 kJ.mol^{-1}; $k_{T_1} = 4.10^{-4}$ g.h^{-1}, $k_{T_2} = 8.2.10^{-3}$ g.h^{-1}) are nearly the same.

The half-life ($t_{1/2}$) of a zero order reaction is expresses as:

$$t_{1/2} = \frac{m_0}{2k} \qquad (27)$$

Where ($m_0 = 0.1207g$) is the initial mass and k is the zero order reaction rate constant. The obtained values are recorded in Table 5.

Table 5: Zero order reaction constant and half-life for aluminium corrosion in 1M HCl

T(K)	k(g.h^{-1})	$t_{1/2}$ (h)
298	0.0004	150.875
318	0.0082	7.360

Temperature has an important effect on the aluminium dissolution in the concerned environment. The greater is the temperature, the greater is the dissolution (see half-life).

Quantum Chemical studies

Global molecular parameters

The calculated molecular parameters of the studied molecule are recorded in Table 5.

Table 5: Molecular and deduced global parameters of NTA using B3LYP/6-31G (d).

Molecular Parameter	value	Molecular Parameter	value
E_{LUMO} (eV)	-1.374	η(eV)	2.7395
E_{HOMO} (eV)	-6.853	σ (eV)$^{-1}$	0.091
ΔE (eV)	5.479	ω (eV)	3.088
μ (Debye)	4.889	ΔN	0.030
μ_p (eV)	-4.1135	E_T (Ha)	-416.985

The fraction of electrons transferred (ΔN) from the inhibitor to the metal was obtained using the equation below:

$$\Delta N = \frac{\phi_{Al} - \chi_{inh}}{2(\eta_{Al} + \eta_{inh})} \qquad (28)$$

Where ϕ_{Al} and η_{Al} are respectively the aluminium work function and hardness whereas χ_{inh} and η_{inh} are the electronegativity and hardness of the studied molecule. The values $\phi_{Al} = 4.28$ eV (Kokalj and Kovacevic, 2011) and $\eta_{Al} = 0$ (Pearson R. G., 1990) were used.

The parameters E_{LUMO} and E_{HOMO} (Musa A. Y. et al., 2010) determine the interactions of the molecule with the other species. HOMO acts as an electron donor whereas LUMO acts an electron acceptor. According to the frontier molecular orbitals theory, highest values of E_{HOMO} and lowest values of E_{LUMO} lead to a good corrosion inhibition character of the molecule. In our work, E_{HOMO} has a high value (-6.856 eV) when compared to values in the literature (Obot I. B. et al., 2009), what shows a trend in electron donation to aluminium's empty orbitals. E_{LUMO} (-1.374 eV) which measures the ability to accept electrons is low when referring to literature (Zarrouk A. et al., 2011). The combined trends of E_{HOMO} and E_{LUMO} justify the low value of ΔE (5.479 eV) indicated by a perusal of the literature.

The dipole moment (μ), which results from the no-uniformity in atomic charges in a molecule is an important molecular parameter. Some authors in the literature (Bereket G.et al., 2002) agreed that the adsorption of a compound with a high dipole moment value on a metal is favoured, while other authors (Kay K. et al., 2016) think that the adsorption is favoured when dipole moment is low. In this work $\mu = 4.8891\ D$ favours adsorption of NTA onto the aluminium surface when taking the good

Citation: Mamadou Yeo et al., 2020. Aluminium corrosion inhibition in 1M HCl by nicotinamide: gravimetric, thermodynamic, kinetic and QSPR studies. Australian Journal of Basic and Applied Sciences, 14(10): 35-47. DOI: 10.22587/ajbas.2020.14.10.5

inhibition efficiency observed in mass loss studies into account. Both chemical absolute hardness (η) and absolute softness (σ) measure the stability or the reactivity of a molecule. So, a high value of chemical hardness (a low value of chemical softness) indicates a resistance towards the deformation or polarization of the electron cloud of the molecule, showing then its stability. A low value of global chemical hardness (η) indicates (Khodaei-Tehranit and Niazi A., 2015) the possibility of the molecule to give or receive electrons. In our case, the value of η (2.7395 eV) and that of σ (0.091 $(eV)^{-1}$) show a good reactivity of NTA.

To bring light on the ability of the molecule to give or receive electrons, the analysis of the electrophilicity index (ω) and the fraction of electrons transferred (ΔN) is necessary. High values of the two parameters indicate the possibility for the molecule to give and receive electrons. Our results (ω = 3.088 eV and ΔN = 0.030) indicate the trend of NTA to receive rather than to give electrons.

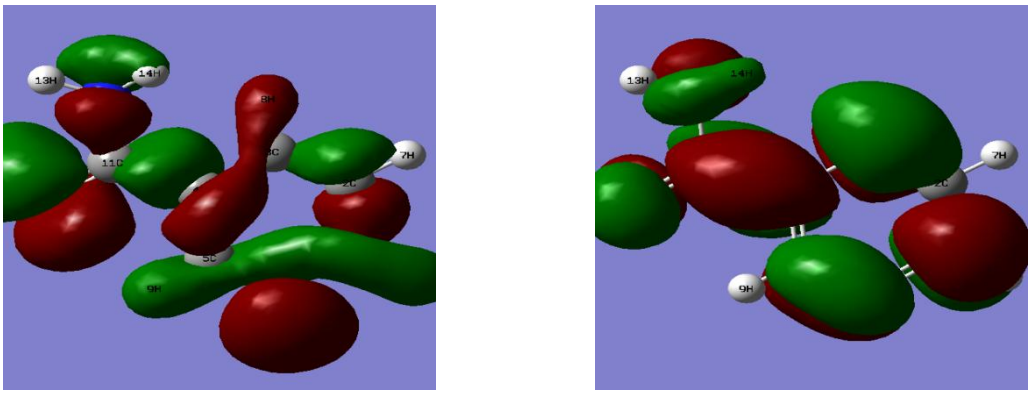
Local reactivity parameters

The condensed Fukui functions (Yang W. and Mortier W. J., 1986) and the dual functions (Chattaraj P. K. et al., 2009) were used to analyse the local reactivity of the inhibitor because they allow determining the nucleophilic and electrophilic sites in the molecule.The determined local parameters are listed in Table 6.

Table 6: Local reactivity functions of NTA using B3LYP/6-31G (d)

Atom	q_{N+1}	q_N	q_{N-1}	f_k^+	f_k^-	Δf_k	$\Delta\omega_k$
1 C	0.008120	0.047388	0.110575	-0.039268	-0.063187	0.023919	0.073862
2 C	-0.087192	-0.143578	-0.140210	0.056386	-0.003368	0.059754	0.184520
3 C	-0.153982	-0.149412	-0.096736	-0.004570	-0.052676	0.048106	0.148551
4 C	**0.034195**	**0.054428**	**0.013508**	-0.020233	**0.040920**	**-0.061153**	**-0.188840**
5 C	0.054032	0.019416	0.111937	0.034616	-0.092521	0.127137	0.392599
6 H	0.004669	0.149629	0.256816	-0.144960	-0.107187	-0.037773	-0.116643
7 H	0.004028	0.144008	0.231041	-0.139980	-0.087033	-0.052947	-0.163500
8 H	0.021808	0.146795	0.222577	-0.124987	-0.075782	-0.049205	-0.151945
9 H	0.059394	0.178846	0.260263	-0.119452	-0.081417	-0.038035	-0.117452
10 N	-0.489735	-0.409548	-0.304439	-0.080187	-0.105109	0.024922	0.076959
11 C	0.389666	0.529968	0.597507	-0.140302	-0.067539	-0.072763	-0.224692
12 N	**-0.639530**	**-0.751966**	**-0.720002**	**0.112436**	-0.031964	**0.144400**	**0.445907**
13 H	0.208810	0.343826	0.406799	-0.135016	-0.062973	-0.072043	-0.222469
14 H	0.209121	0.332569	0.387653	-0.123448	-0.055084	-0.068364	-0.211108
15 O	-0.623404	-0.492369	-0.337290	-0.131035	-0.155079	0.024044	0.074248

To characterize a site towards a nucleophilic or an electrophilic attack in a molecule, it is necessary (Morell C. et al., 2006) to use the sign of the dual descriptors. According to the literature (Gazquez J. 1997), if $\Delta f_k > 0$, the site is favoured for a nucleophilic attack, whereas if $\Delta f_k < 0$, the site is favoured for an electrophilic attack.
Fig. 11 gives the HOMO and LUMO orbitals of Nicotinamide



HOMO LUMO

Fig. 11: Frontier molecular orbitals (FMO) of NTA using B3LYP/6-31G (d)

Citation: Mamadou Yeo et al., 2020. Aluminium corrosion inhibition in 1M HCl by nicotinamide: gravimetric, thermodynamic, kinetic and QSPR studies. Australian Journal of Basic and Applied Sciences, 14(10): 35-47. DOI: 10.22587/ajbas.2020.14.10.5

The preferred sites for electrophilic attack and nucleophilic attack in Nicotinamide, are respectively C (4) with large negative values of Δf and $\Delta\omega$ and N (12) with large positive values of Δf and $\Delta\omega$.

QSPR studies

Attempts have been made to establish a mathematical relation (Lukovits et al., 2003) between inhibition efficiency and some sets of reactivity parameters: (E_{HOMO}, E_{LUMO}, ΔE), (E_{HOMO}, E_{LUMO}, μ), (E_{HOMO}, E_{LUMO}, ω) and (E_{HOMO}, ΔE, ω). Figure 12 A to D give the plots of IE_{Theo} (%) versus IE_{Exp} (%).

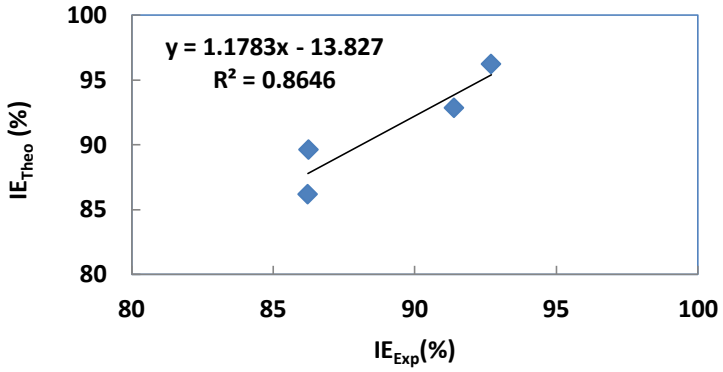


Fig. 12 A: IE_{Theo} (%) versus IE_{Exp} (%) for the set of parameters (E_{HOMO}, E_{LUMO}, ΔE)

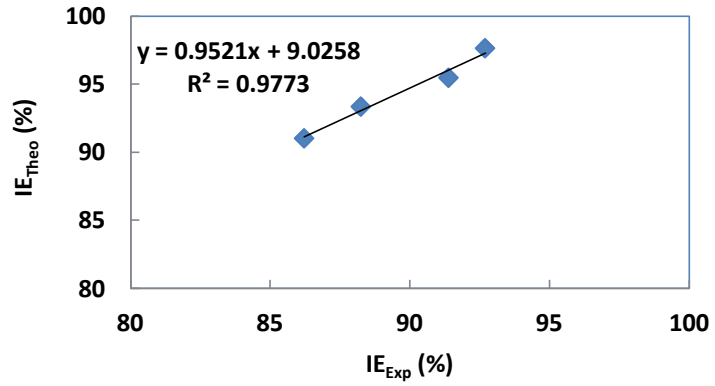


Fig. 12 B: IE_{Theo} (%) versus IE_{Exp} (%) for the set of parameters (E_{HOMO}, E_{LUMO}, μ)

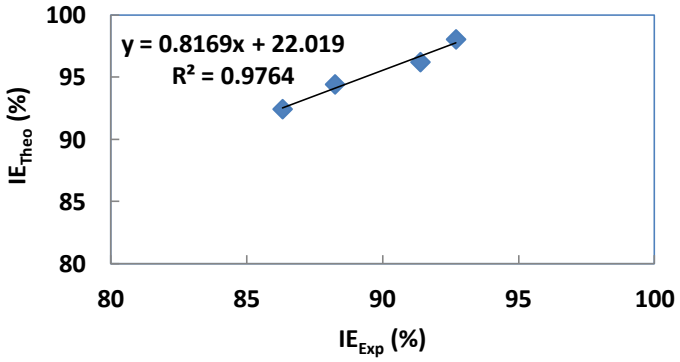


Fig. 12 C: IE_{Theo} (%) versus IE_{Exp} (%) for the set of parameters (E_{HOMO}, E_{LUMO}, ω)

Citation: Mamadou Yeo et al., 2020. Aluminium corrosion inhibition in 1M HCl by nicotinamide: gravimetric, thermodynamic, kinetic and QSPR studies. Australian Journal of Basic and Applied Sciences, 14(10): 35-47. DOI: 10.22587/ajbas.2020.14.10.5

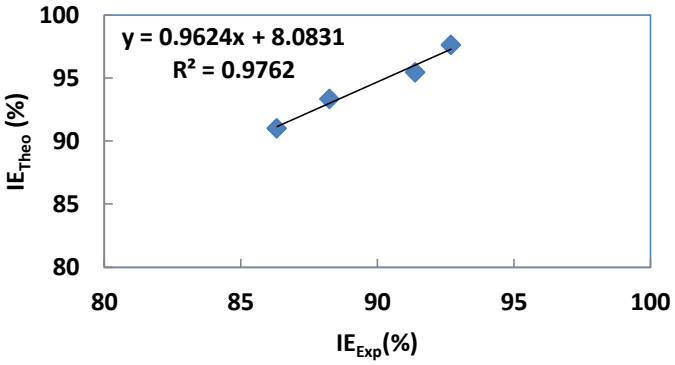


Fig. 12 D: IE_{Theo} (%) versus IE_{Exp} (%) for the set of parameters (E_{HOMO}, ΔE, ω)

The best set of parameters was choosen, using correlation coefficient (R^2) and a statistical analysis based on the sum of squared errors:

$$SSE = \sum\left[IE_{Theo}(\%) - IE_{Exp}(\%)\right]^2 \qquad (29)$$

The coefficients of the model and the values of SSE are listed in Table 4.

Table7: coefficients A, B, D and E, correlation coefficients (R^2) and the values of SSE.

Set of parameters	A	B	D	E	R^2	SSE
(E_{HOMO}, E_{LUMO}, ΔE)	750.851	7459.696	-625.193	18820.683	0.8646	14.5
(E_{HOMO}, E_{LUMO}, μ)	1718.408	13108.311	10492.369	-21511.094	0.9776	90.1
(E_{HOMO}, E_{LUMO}, ω)	1490.580	6720.303	$6.466.10^{13}$	$-1.967.10^{14}$	0.9764	126.70
(E_{HOMO}, ΔE, ω)	460.473	$-2.428.10^{13}$	$7.947.10^{13}$	$-1.123.10^{14}$	0.9762	89.35

Observing Table 7, one can see that (E_{HOMO}, E_{LUMO}, μ) with (R^2 = 0.9776, SSE = 90.1) and (E_{HOMO}, ΔE, ω) with (R^2= 0.9762, SSE = 89.35) are the best sets.

CONCLUSION

The mass loss method shows that Nicotinamide is a good inhibitor for the aluminium corrosion in 1M HCl. The inhibition efficiency increases with increasing concentration, but decreases with increasing temperature. The thermodynamic parameters obtained indicate that physisorption mechanism is preponderant. The inhibitor adsorbs onto the aluminium surface according to the Villamil adsorption isotherm. The kinetics of the aluminium dissolution, both in the in the presence or in the absence of the NTA is zero order. Global molecular parameters as E_{HOMO}, E_{LUMO}, ΔE and μ, confirmed that NTA is a good inhibitor for aluminium corrosion in the studied environment. From the local reactivity indices, it was found that the site for electrophilic attack is C (4), whereas the site for nucleophilic attack is N (12). Quantitative Structure Property Relationship approach was used to correlate some sets of reactivity parameters with the NTA inhibition efficiency.

BIBLIOGRAPHY

Abdallah M., **2004**. *Antibacterial drug as corrosion inhibitors for corrosion of Aluminium in hydrochloric acid solution*, Corrosion Science, 46, 1981-1996.

Abdallah M., Zaafarany I., Al-Karance S. O., Abd El-Fattah, A. A. **2012**. *Antihypertensive drugs as inhibitors for corrosion of aluminium and aluminium silicon alloys in aqueous solutions*, Arabian Journal of Chemistry, 5, 225-234.

Adejo S. O., Ekwenchi M. M.**2014**.*Proposing a new empirical adsorption isotherm known as Adejo-Ekwenchi isotherm*, IOSR Journal of Applied Chemistry, 6, 66-77.

Ameh P. O., Sami U. M. 2015. *Cefuroxime Axetil: A commercially Available Pro-Drug as corrosion Inhibitor for Aluminium in Hydrochloric Acid Solution*, *Journal of Heterocyclics*, 1, 1-6.

Badiae A. M., Mohana K. N.**2009**. *Effect of temperature and fluid on corrosion mechanism of low carbon steel in presence of 2-hydrazino-4, 7- dimethylbenzothiazole in industrial water medium*, 51 (9), 2231-2241.

Bereket G, Hür E, Ogretir C. **2002**. *Quantum chemical studies on some imidazole derivatives as corrosion inhibitors for iron in acidic medium*. J Mol Struc Theochem 578, 79-88.

Chattaraj, P. K., Maiti, B., Sarkar, U. *J.* **2003.** *Philicity: A unified Treatment of Chemical Reactivity and Selectivity*, Phys. Chem. A., 107, 25, 4973-4975.

Chattaraj P. K., Chakraborty A., Giri S. **2009**. *Net Electrophilicity*, the Journal of Physical Chemistry A 113, 10068–10074.

Davis J. R. **1999**. *Corrosion of aluminium and aluminium alloys*, ASM International, Materials Park.

Ebenso E. E., Obot I. B. **2010**. *Inhibitive properties, Thermodynamic Characterization and Quantum Chemical Studies of Secmidazole on mild steel corrosion in Acid Medium*, Int. J. Electrochem. Sci., 5, 2012-2035.

Eddy N. O., Momoh-Yahaya H. Oguzie E. E. **2015**.*Theoretical and experimental studies on the corrosion inhibition potentials of some purines for aluminium in 0,1M HCl*, J. Adv. Res. 6, 203-217.

Citation: Mamadou Yeo et al., 2020. Aluminium corrosion inhibition in 1M HCl by nicotinamide: gravimetric, thermodynamic, kinetic and QSPR studies. Australian Journal of Basic and Applied Sciences, 14(10): 35-47. DOI: 10.22587/ajbas.2020.14.10.5

Frisch M.J., Trucks G.W., Schlegel H.B., Scuseria G.E. Robb M.A., Cheeseman J.R., Scalmani G., Barone V., Mennucci B., Petersson G.A., Nakatsuji H., Caricato M., Li X., Hratchian H.P., Izmaylov A.F., Bloino J., Zheng G., Sonnenberg J. L., Hada M., Ehara M., Toyota K., Fukuda R., Hasegawa J., Ishida M., Nakajima T., Honda Y., Kitao O., Nakai H., Vreven T., Montgomery J. A., Jr., Peralta J. E., Ogliaro F., Bearpark M., Heyd J. J., Brothers E., Kudin K.N., Staroverov V.N., Kobayashi R., Normand J., Raghavachari K., Rendell A., Burant J.C., Iyengar S.S., Tomasi J., Cossi M., Rega N., Millam J.M., Klene M., Knox J.E., Cross J.B., Bakken V., Adamo C., Jaramillo J., Gomperts R., Stratmann R.E., Yazyev O., Austin A.J., Cammi R., Pomelli C., Ochterski J.W., Martin R.L., Morokuma K., Zakrzewski V.G., Voth G.A., Salvador P., Dannenberg J.J., Dapprich S., Daniels A.D., Farkas Ö., Foresman J.B., Ortiz J.V., Cioslowski J., Fox D.J. **2009**. *Gaussian 09 (Gaussian, Inc., Wallingford CT).*

Fouda S., Abd-El-Aal A., Khandil A. B. **2006**. *The effect of some phthalimide derivatives on corrosion behaviour of copper in nitric acid*, Desalination, 201, 216-223.

Gazquez J. L. **1997**. *The hard and soft acids and bases principle*, The Journal of Physical Chemistry A, 101, 26, 4657-4659.

Geerlings P., De Proft F., Langenaeker W. **2003**. *Conceptual Density Functional Theory*, Chemical Reviews 103, 1793–1873.

Kay K, Senthilkumar A.N., Tharini K. **2016**. *Quantum chemical study on the corrosion inhibition of N-benzylpiperidine-4-one Oxime*. Adv Appl Sci Res 7: 150-154.

Khaled, K.F., Al-Qahtani, M.M. **2009**. *The inhibitive effect of some tetrazole derivatives towards Al corrosion in acid solution: chemical electrochemical and theoretical studies*. Mater. Chem. Phys.113, 150–158.

Khodaei-Tehrani M, Niazi A. **2015**. *Quantum chemical studies on the corrosion inhibition of some hector bases on mild steel in acidic medium*. Oriental Journal of Chemistry 31, 423- 429.

Kokalj A. and Kovacevic N. **2011.** *On the consistent use of electrophilicity index and HSAB-based electron transfer and its associated change of energy parameters*, Chemical Physics Letters, 507, 181–184.

Kumar S. H., Karthikeyan S. **2012**. *Inhibition of mild steel corrosion in hydrochloric acid solution by Cloxacillin drug*. Journal of Materials and Environmental Science, 3, 925-934.

Morell C., Grand A., Toro-Labbé A. **2005**. *New Dual Descriptor for Chemical Reactivity*, J. Phys. Chem. A, 109, 205-212.

Musa A.Y., Kadhum A.H., Mohamad A.B., Rohma A.B., Mesmari H. **2010**. *Electrochemical and quantum chemical calculations on 4, 4-dimethyloxazolidine-2-thione as inhibitor for mild steel corrosion in hydrochloric acid*, J Mol. Struct. 969: 233-237.

Naqui I., Salemi A.R., Naveed S. **2011**. *Cefixime: A drug as efficient corrosion inhibitors for mild steel in acidic media. Electrochemical & Thermodynamic studies* International Journal of Electrochemical Science 6, 146-161.

Obi-Egbedi, N. O., Obot I. B. **2011**. *Inhibitive properties, Thermodynamic and quantum chemical studies of alloxazine on mild steel corrosion in H_2SO_4*, 53, 263-275.

Obot, I.B., Obi-Egbedi, N.O., Umoren, S.A. **2009**. *Adsorption characteristics and corrosion inhibitive properties of clotrimazole for aluminium corrosion in hydrochloric acid*. Int. J. Electrochem. Sci. 4, 863–877.

Obot I. B., Obi-Egbedi N. O., Umoren S. A. **2009**. *The synergistic inhibitive effect and some quantum chemical parameters of 2, 3- diaminonaphtalène and iodide ions on the hydrochloric acid corrosion of aluminium*. Corros. Sci. 51, 276-282.

Pearson R.G. **1990**. *Hard and soft acids and bases-the evolution of a chemical concept*, Coordination Chemistry Reviews, 100, 403–425.

Polnear I. J**. 1995**. *Light alloys: Metallurgy of light metals*; *3rd Ed.*, Arnold London.

Sahin M., Bilgic S., Yilmaz H. **2002**. *The inhibition effects of some cyclic nitrogen compounds on the corrosion of steel in NaCl mediums*, Appl. Surf. Sci. 195, 1-7.

Singh A.K., Quraishi M.A. **2010**. *Effect of Cefazolin on the corrosion of mild steel in Hydrochloric acid solution*, Corrosion Science, 52,152-160.

Singh A.K., Singh S.K., Ebenso E.E. **2011**. *Cefacetrile as corrosion inhibitors for mild steel in acidic media*, International Journal of Electrochemical Science, 6, 5689- 5700.

Umoren S. A., Obot I. B., Ebenso E. E., Okafor P. C., Ogbode O., Oguzie E. E. **2006**. *Gum Arabic as a potential corrosion inhibitor for aluminium in alkaline medium and its adsorption characteristics*, 53, 277-282.

Villamil R. F.V., Corio P., Rubin J. C., Agostinho S.M.L.**1999**. *Effect of sodium dodecylsulfate on copper corrosion in sulphuric acid media in the absence and presence of benzothiazole*, 472, 112-119.

Yang W., Mortier W. J. **1986**. *The use of global and local molecular parameters for the analysis of the gas-phase basicity of amines*. J. Am. Chem. Soc. 108, 5708-5711.

Zarrouk A., Hammouti B., Zarrok H., Warad I., Bouachrine M. **2011**. *N containing organic compound as an effective corrosion inhibitor for copper in 2M HNO_3: Weight loss and quantum chemical study*, Der Pharma Chemica 3, 263-271.